Chapter 7

Photoelectron Diffraction in Magnetic Dichroism: Experiment

In this chapter we present the results of an investigation of the angular dependence of magnetic linear dichroism in photoemission from the 4f shells of rare-earth metal single crystalline surfaces. This work was motivated by earlier studies of magnetic rare-earth surfaces by means of MD in core-level PE [43,57]. We find that the MD signals in 4f PE from single-crystalline surfaces exhibit a quite spectacular variation with the emission angle that can be understood as a manifestation of photoelectron diffraction in the photoemission final state.

7.1 Gd(0001)

The spectra of the 4f-line multiplet of the Gd(0001) surface, recorded with linearly polarized light for two opposite magnetization directions in the experimental geometry given in Fig. 3.8, show the well-known changes upon magnetization reversal due to the dichroic effect [10,76]. In addition, the shape of the 4f spectrum is strongly modified with a variation of the emission angle. This is shown in Fig. 7.1, where three pairs of spectra (for emission angles $\alpha = -2.46°$, $0°$, and $2.46°$) represent three characteristic cases. The zero angle (normal emission) was defined with an accuracy of $\Delta\alpha = \pm 0.5°$. One can see that the spectral shape of the bulk component changes with emission direction from peak-shaped to rounded (similar to the shapes corresponding to $\Delta M = +1$ and $\Delta M = -1$ transitions given in the inset of the Fig. 5.2), even without changing the sample magnetization.

The systematic variation of the 4f-MLD signal of the Gd(0001) surface is shown in Fig. 7.2 as a 3D-plot of the 4f spectral intensity difference for opposite sample magnetizations versus binding energy, with the emission angle as parameter. Spectra taken at the same off-normal emission angles but from different sides with respect to normal emission are marked by the same color; black correspond to surface normal. From previous considerations we expect two components also in this MLD signal resulting from (not fully resolved) sur-

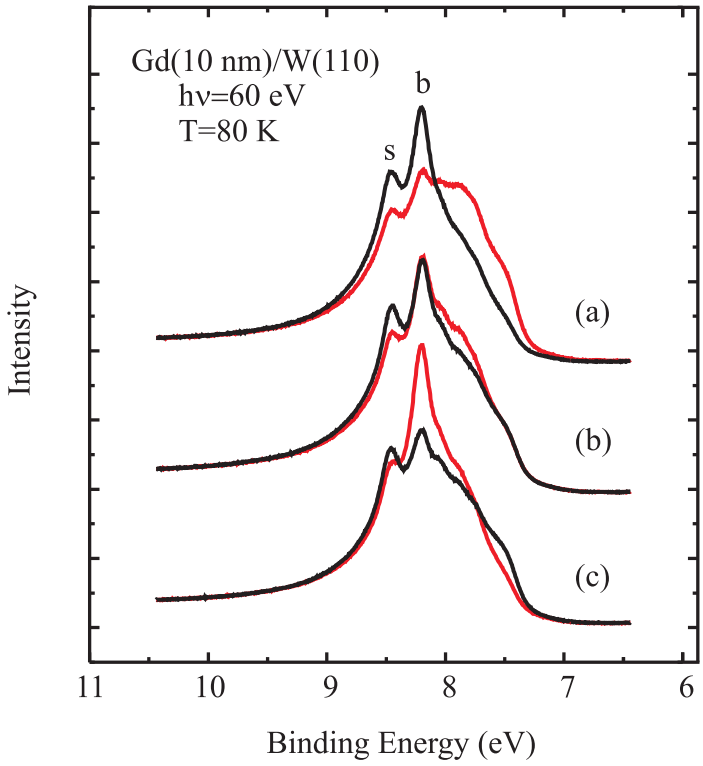

Figure 7.1: Photoemission spectra of the Gd(0001) 4f multiplet recorded with $\theta^{h\nu} = 35°$ for different emission angles: (a) -2.46°, (b) 0°, (c) +2.46°. Pairs combine spectra for opposite magnetization directions (red and black curves) in the experimental geometry shown in Fig. 3.8.

face and bulk components, shifted in binding energy due to the surface core-level shift (similar to Fig. 5.2). One can indeed recognize the shifted components in the spectra at negative values of the emission angle α (see Fig. 7.2). However, even without a detailed analysis one can see that the relative intensities of surface and bulk components change rapidly with the emission angle. At normal emission, only the surface component is clearly recognized in the MLD spectrum. For positive emission angles, the shape of the MLD signal does not resemble the typical form of the Gd 4f MD spectra any more (compare with e.g. Fig. 5.2). A closer look at the spectra allows one to suppose that the observed changes in shape with emission angle could be due to a sign reversal of the bulk component.

The sum of the 4f spectra for opposite magnetizations, representing the even parts of the spectra with respect to magnetization (the nonmagnetic contribution, see Section 4.4) are shown in Fig. 7.3. They clearly indicate that the dramatic variations in the MLD spectra are not accompanied by similarly

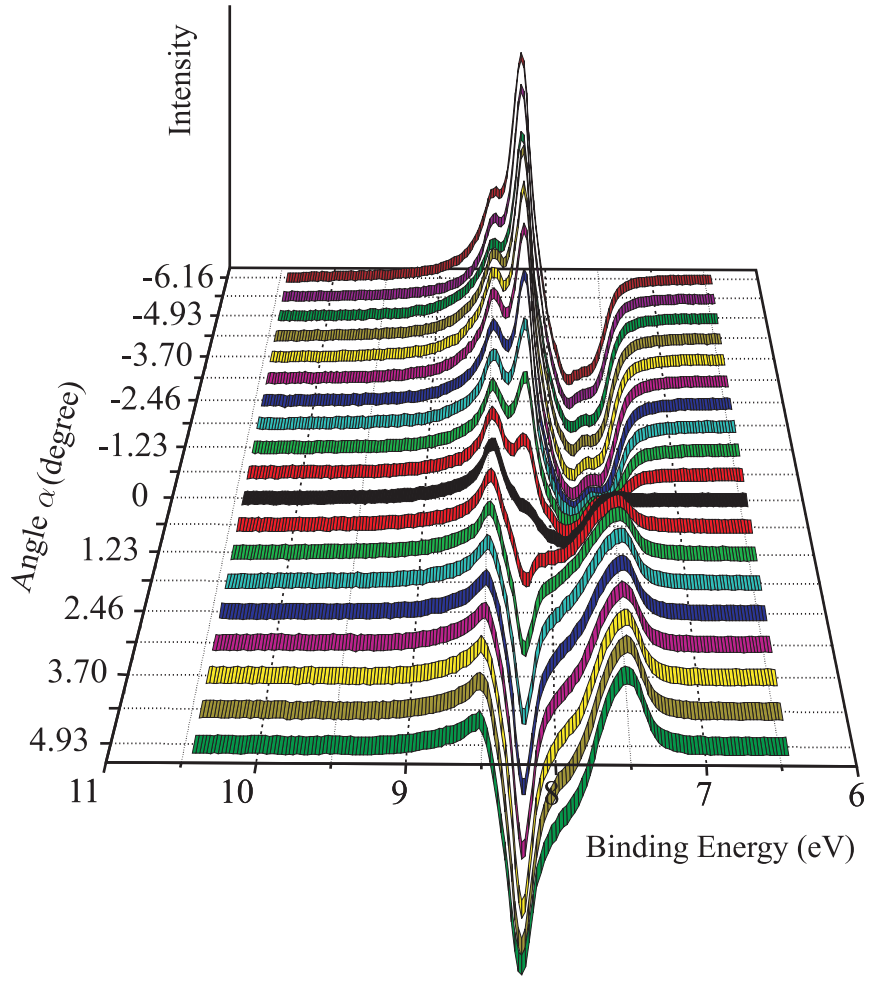

Figure 7.2: Set of photoemission MLD spectra (showing the angular variation of the Gd 4f MD signal with the emission angle around normal emission, recorded with a constant angular step of 0.62° between the individual spectra. Spectra with the same value of emission angle, but from opposite sides with respect to the surface normal, were marked by the same color; the normal-emission spectrum is shown in black.

large changes in the non-magnetic components: shapes and intensities of the 4f spectra nearly constant over the presented angular range.

This behavior of the surface and bulk MD components in Fig. 7.3 can be attributed to diffraction, affecting the outgoing photoelectron waves. The strong angular variation of the bulk MD component and the much weaker variation of the surface component are most likely caused by the fact that the photoelectron wave emitted from surface atoms can undergo only backscattering, so that photoelectron diffraction is much weaker than for a photoelectron wave originating from a bulk atom. By contrast, diffraction and interference of the photoelectron waves excited in the bulk can be very large [74]. According to

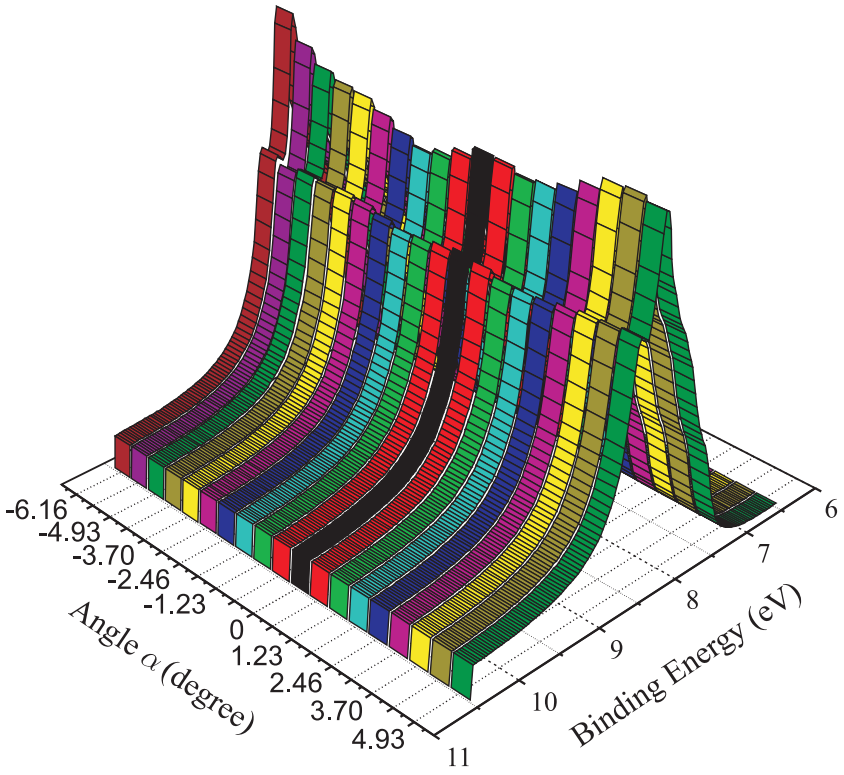

Figure 7.3: Set of sum spectra that represent the non-magnetic components in the Gd 4f photoemission spectra, supplementing the set of spectra presented in Fig. 7.2 (same color code).

the model considered above, the MD effect can be separated into atomic and diffraction parts. From this model one would expect to observe atomic dichroism along low index directions, while for emission directions in between one expects to observe diffraction dichroism. In the MD spectrum for $\alpha = -6^\circ$, the amplitude of the bulk component dominates over the surface component by half an order of magnitude. If we attribute the MD signal of the bulk component to the diffraction dichroism and the MD of the surface component mostly to the atomic MD (giving an upper limit for atomic dichroism), we come to the conclusion that diffraction dichroism dominates over the atomic MD in the present case. The zero crossing of the bulk component at normal emission, where one would expect to see the atomic part of MD, points to the absence of an atomic dichroism at this photon energy. However, the rapidly changing (and dominating) diffraction component does not allow us to strictly exclude the presence of an atomic part (due to the $\Delta\alpha = \pm 0.5^\circ$ accuracy of adjustment of the crystal surface normal with respect to the analyzer). Yet, one can state that there is a strong dominance of diffraction dichroism over the atomic one. Note that one expects diffraction contributions also for the surface component, due to backward scattering from the periodic atomic structure of subsurface layers (in particular at the rather low kinetic energies in the present experiment).

The reason why diffraction dichroism dominates over the atomic one becomes clear from the photon energy dependence of the squared transition matrix elements defining transition probabilities for excitation from the f shell to the d and g continuum (see Appendix B, Fig. B.1). At 60-eV photon energy, the transition probability for the $f \rightarrow g$ channel is higher by a factor of twenty as compared to the $f \rightarrow d$ channel. This means that practically only g waves are excited, with the direct consequence that the atomic dichroism vanishes, since it originates from the interference of excited d and g waves. By contrast, diffraction dichroism remains as it arises from an interference of g waves.

In order to obtain a clear insight into the observed angular dependences of the MLD signal, we applied a fitting procedure to the experimental spectra. Figure 7.4 represents the deconvolution of the Gd-4f MLD signal from the spectra given in Fig. 7.1. We see that the sign of the magnetic spectrum, I_1, is the same for the surface and bulk components for $\alpha = -2.46°$ (Fig. 7.4(a)), although the amplitudes are different by a factor of two. For normal emission, the description of the signal requires only the surface component, as shown in Fig. 7.4(b) (magnified by a factor of two). For the emission direction $\alpha = +2.46°$ (Fig. 7.4(c)), the bulk component has clearly reversed its sign, resulting in a quite uncommon shape of the overall 4f-line MLD signal (two nodes instead of the expected one, as for normal emission).

The theoretical description of dichroism in photoemission from 4f shells is far from being simple [32, 34]. In particular, when modeling the angular behavior of the PE intensity at a crystal surface, which is subject to strong diffractions effects, an extensive computer code would be required. To describe scattering and multiple scattering of $f \rightarrow g$ and $f \rightarrow d$ transitions and interference, one would in addition have to incorporate atomic multiplet calculations into a diffraction code like EDAC [77]; currently this is not available [78]. Nevertheless, we can appreciate the role of diffraction effects in the observed angular behavior, including the sign reversal at normal emission, from a comparison with the simple model described above, and with the Fe $2p$ case.

For a simple qualitative discussion, we have used the results of photoelectron diffraction calculations performed with the EDAC computer code developed by F. Javier Garcia de Abajo [77]. The code allows one to calculate photoelectron diffraction in the multiple scattering approach for a big cluster (a few hundred atoms). Unfortunately, it does not allow one to directly include the dichroic effects into the dipole transition matrix elements (details can be found in Ref. [77]). Yet, one can try to include them at a later stage using the calculated photoelectron waves as a basis set to derive the photoemission line intensities. This works well for fully occupied shells using the configuration interaction approach, as was we shown in Section 4.2. Yet, a description of open shells is more complicated [39, 79] and no computer code exists at present.

Let us consider the intensity of photoelectron waves originating from atoms in different layers, derived in the multiple-scattering approach for a cluster (of about 200 atoms) simulating the (0001) surface of an hcp lattice, with the atomic parameters chosen for gadolinium and the geometry corresponding to the experiment (Fig. 3.8). The $|j; m_j\rangle$ states represent a full basis set and, in general, one could use them to construct particular photoemission final states.

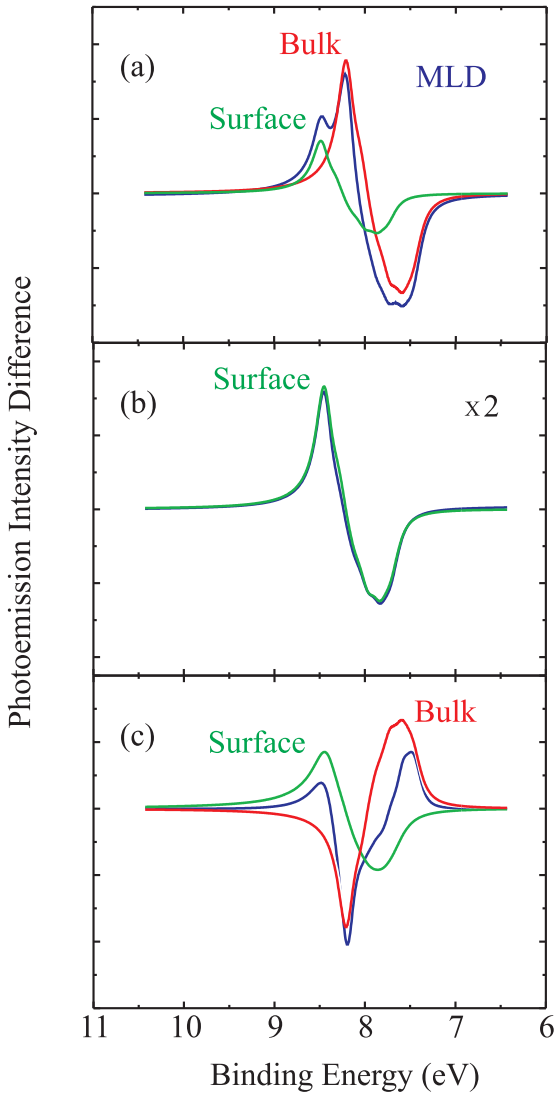

Figure 7.4: Deconvolution of the dichroic signals into bulk and surface components derived from the spectra shown in Fig. 7.1 : (a) $-2.46°$ - both component have the same sign; (b) $0°$ - only the surface component is observed; (c) $+2.46°$ - the bulk component reverses its sign. Bulk component: red; surface component: green; experimental spectra: blue.

Therefore, one can take the angular dependence of $|j; m_j\rangle$ to predict the intensity variation of the Gd-4f spectrum with the emission angle.

The layer-resolved photoemission intensity from a $\left|\frac{7}{2}; -\frac{7}{2}\right\rangle$ and a $\left|\frac{5}{2}; -\frac{5}{2}\right\rangle$ state, calculated as a function of emission angle is presented in Fig. 7.5. One sees that the intensity variation as function of the angle α for both states is almost the same (as well as in the rest of the basic set functions); it is rather defined by the positions of the atoms in the lattice. The intensities of the

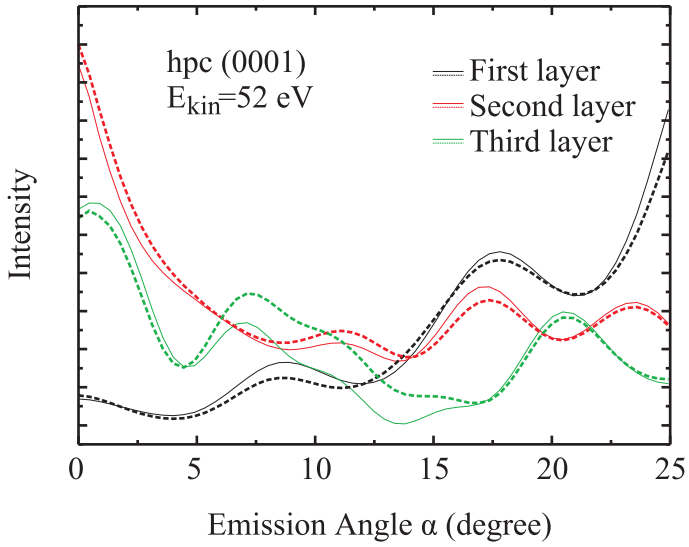

Figure 7.5: Results of layer-resolved photoemission intensity calculations to simulate emission from the 4f shell. The calculations made use of the EDAC computer code including multiple scattering in a cluster of about 200 atoms simulating an hcp(0001) surface. The photoelectron kinetic energy was $E_{kin} =$ 52 eV; $\left|\frac{7}{2};-\frac{7}{2}\right\rangle$ states (solid lines), $\left|\frac{5}{2};-\frac{5}{2}\right\rangle$ states (dashed lines).

photoelectron waves originating from atoms located in the second (subsurface) layer and in the third layer yield an interference maximum at normal emission. By contrast, when the emitting atom is in the surface layer, there is no such pronounced maximum. In the two-atom cluster model, considered in Section 6.1, we have seen that the total intensity reaches its maximum at directions corresponding to a zero phase shift (zero-order interference peak) and that the MD signal reverses sign. We find the same behavior for the Gd(0001) 4f spectrum, i.e. a maximum of the total intensities at normal emission for the two subsurface layers. Therefore, we are led to expect a sign reversal of the diffraction MD signal at normal emission. Even though the subsurface atom does not have an on-top neighbor for scattering at the (0001) surface of the hcp lattice, waves diffracted from surrounding atoms located symmetrically will have zero phase shift for the normal-emission angle. From the absence of such a maximum in the surface-layer emission, we expect no sign reversal in the corresponding diffraction MD signal. The predicted behavior, derived in a semi-qualitative way, agrees perfectly with the observed experimental behavior of the Gd(0001) surface and the bulk 4f PE component.

By simultaneous fitting of the whole angular series one could extract angular dependences of the MD intensities of the surface and bulk components. However, such a procedure is hardly feasible due to the incompletely resolved complex structure of the Gd-4f multiplet components. Without quantitative theoretical description to be compared with, there is no idea to extract such

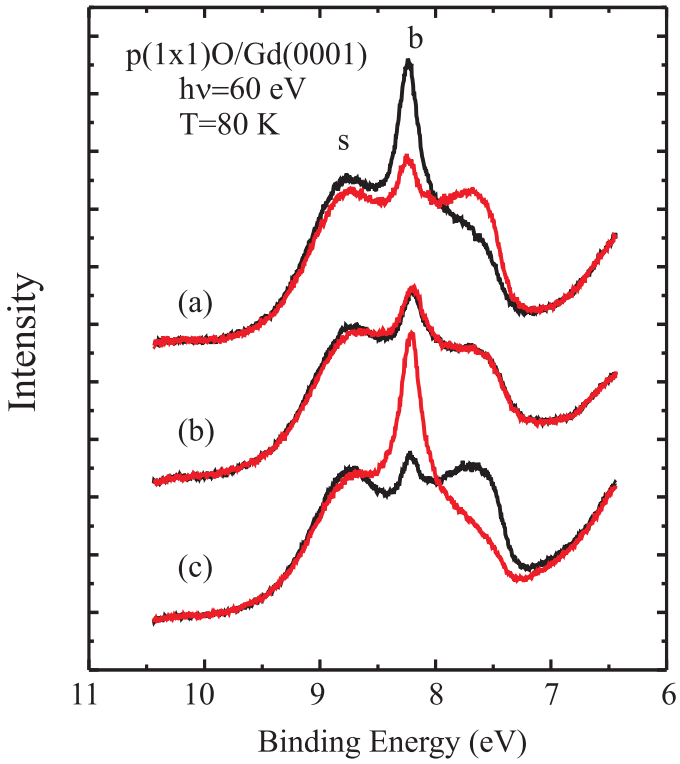

Figure 7.6: PE spectra of the Gd 4f multiplet recorded for $\theta^{h\nu} = 35°$ with linearly polarized light for the $p(1\times1)O/Gd(0001)$ surface at different emission angles: (a) -4.93°, (b) 0°, (c) +4.93°. The spectra corresponding to opposite magnetization directions (red and black curves) are combined in pairs according to the emission angle (experimental error bars were $\Delta = \pm 0.5°$).

detailed information in such a complicated case. Instead, we search for another system that may provide clear and direct insight into the interplay of the MLD signal and diffraction in photoemission from the 4f shell.

7.2 $p(1\times1)O/Gd(0001)$

To get access to the angular behavior of the bulk component, one needs to separate the surface and bulk signals. Oxygen adsorption on the Gd(0001) surface leads to a suppression of the surface magnetic order, as was described in Section 5.2, and consequently to the disappearance of the surface MD signal. Hence, the $p(1\times1)O/Gd(0001)$ surface monoxide allows a direct observation of the angular behavior of the bulk Gd-4f PE component.

Figure 7.6 shows pairs of 4f spectra of $p(1\times1)O/Gd(0001)$ for three different emission angles and opposite magnetization directions. For the middle pair, corresponding to $\alpha = 0°$, the spectra perfectly match (Fig. 7.6(b)), owing to the absence of a surface MD component (no difference between red and

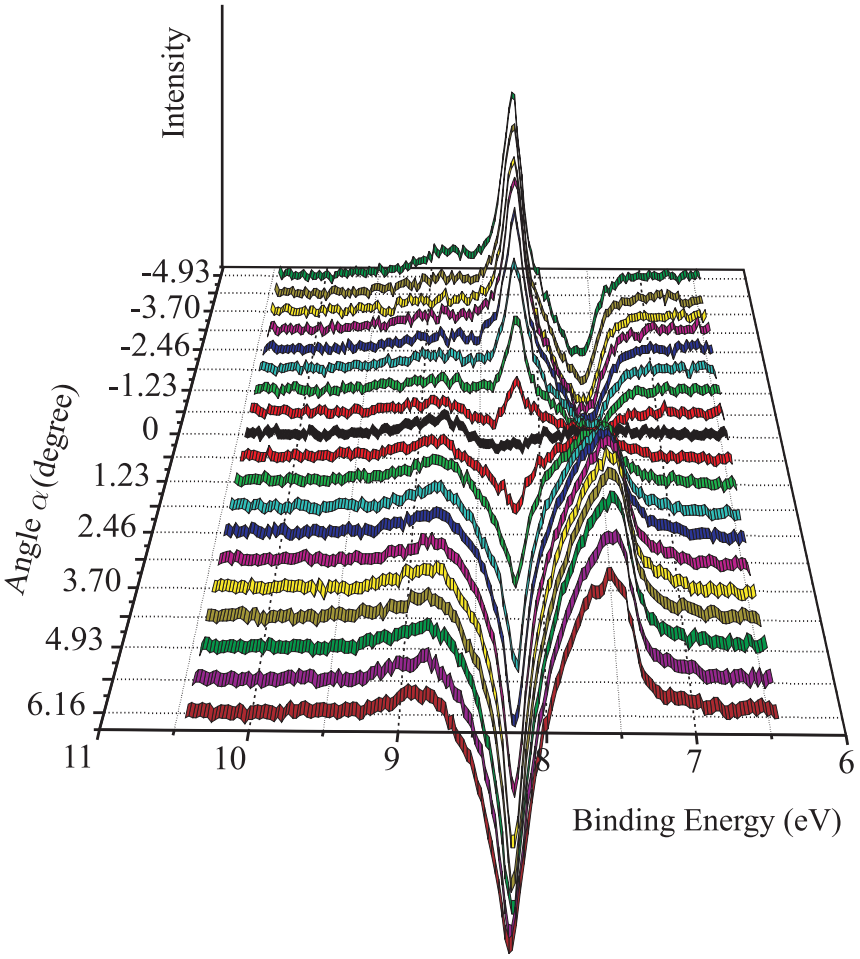

Figure 7.7: Experimental 4f-PE MLD spectra of the $p(1\times1)O/Gd(0001)$ surface. The emission angles are given with respect to the surface normal (constant angular steps of 0.62°). Spectra with the same modulus of emission angle, but from opposite sides with respect to the surface normal, are marked by the same colors; normal emission is marked as black.

black spectra in (b)) and clear vanishing of MD for the bulk component at normal emission, similar to the case of a clean Gd(0001) surface. The pairs corresponding to off-normal emission clearly show that the MD signal of the bulk component reverses sign upon crossing the surface normal (see Fig. 7.6 (a) and (c)).

Figure 7.7 shows the full data set of MD spectra of the $p(1 \times 1)O/Gd(0001)$ 4f multiplet around normal emission in a analogous way as in the previous case of Gd(0001). The bulk component varies strongly with emission angle, crossing zero near the surface normal. A little trace of the surface component can be recognized from the high-binding-energy side of the 4f spectra. Inspection of the even part of the spectra, derived by summing the pairs of spectra but with opposite magnetization with the same emission angle, indicates again rather

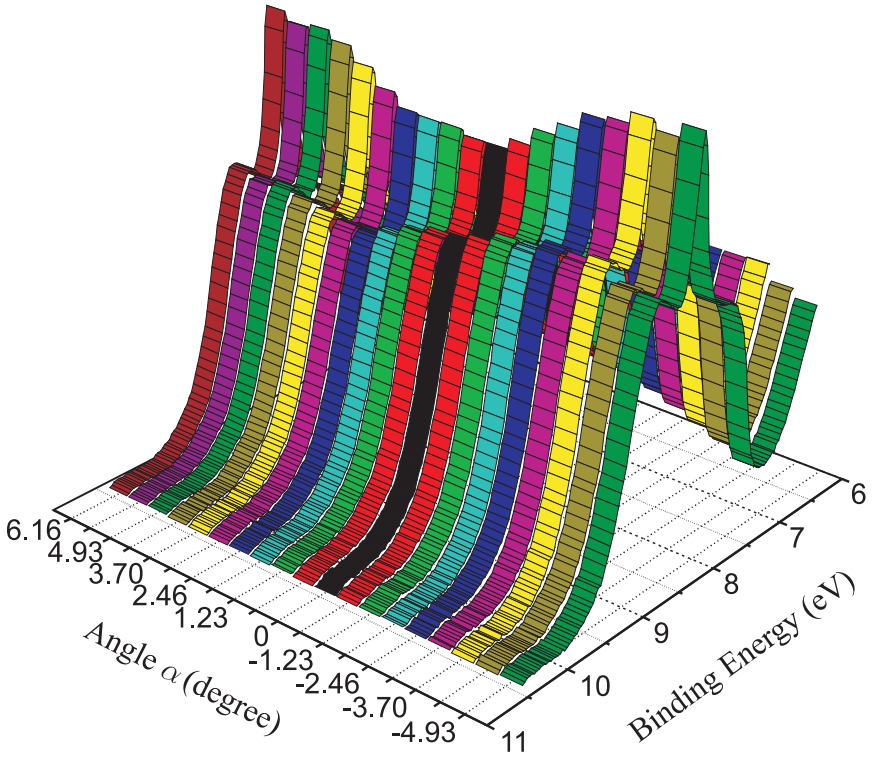

Figure 7.8: Corresponding sums of the Gd-4f PE spectra from $p(1 \times 1)O/Gd(0001)$, revealing a minor variation of the non-magnetic components with emission angle. The same color code for the emission angle α was used as in Fig. 7.7.

small variations in the intensities; this is illustrated in Fig. 7.8.

The two MD spectra recorded at emission angles of $\alpha = +4.93°$ and $\alpha = -4.93°$ are shown in Fig. 7.9. To compare the shapes of the MD signals, the sign of the spectrum taken at $\alpha = 4.93°$ was reversed. Obviously, the spectral shapes are (i) quite similar and (ii) closely resemble the shape of the I^1 fundamental spectrum considered above (see Section 4.4). The bulk component is clearly dominating over the very weak surface component. However, it is easy to see that, the surface signal does not reverse its sign, in contrast to the bulk component.

It is straightforward to derive the peak-to-peak amplitude from pairs of spectra recorded for the same $|\alpha|$, after multiplying one of them by (-1) as shown in Fig. 7.9. Figure 7.10 presents the angular dependence of this peak-to-peak amplitude of the bulk component (red curve). Summing up the pairs of MD spectra with the same absolute value of α eliminates possible contributions from the surface component, inherently assuming a symmetrical angular behavior of the surface component. When, by contrast, one plots the peak-to-peak amplitudes of the raw spectra - without adding up pairs with the same $|\alpha|$ - one obtains the black curve in Fig. 7.10. The slight shift with respect to

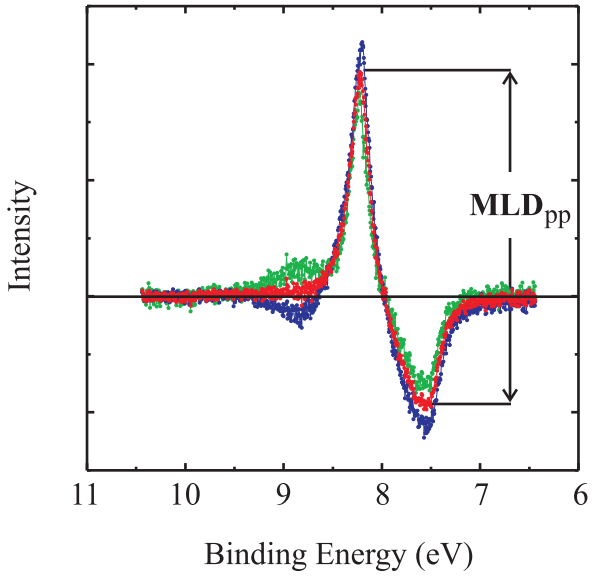

Figure 7.9: MLD spectra of the Gd-4f multiplet taken for emission angles of $\alpha = +4.93°$ (blue) and $\alpha = -4.93°$ (green); the spectra were selected from the angular series shown in Fig. 7.7. For comparison, the sign of the spectrum corresponding to $\alpha = +4.93°$ has been reversed (blue), with the average of the two spectra represented by the red curve.

the symmetrized curve (red) is due to the residual surface contribution that is not fully separated in energy (see Fig. 7.9). The difference between the angular dependence curves in Fig. 7.10 may serve as an upper limit for the expected atomic MD contribution (expecting its manifestation as a rigid shift of the MD curve with respect to the zero line, see Chapter 6).

The very strong modification of the MD angular behavior predicted by atomic multiplet theory becomes evident from the observed behavior of the bulk component; the angular behavior expected for a free atom is plotted for comparison. Its amplitude was normalized to the typical value observed in MCD photoemission experiments. Fitting of the MLD$_{pp}$ curve with the sinus function gives an oscillation period of 18°. This period corresponds to the variation, which one would expect from our simple model. Indeed the model predicts the sign reversal of the diffraction MD signal as the emission angle crosses the direction connecting the emitting and the scattering atom. For the angular scan in the plane defined by the surface normal and the b-axis in the (0001) plane of the hcp lattice (between n.n. atoms) one can find that 17.4° is the smallest angle, connecting the atoms in the layers separated by one layer (see Fig. 7.11). This is in perfect agreement with the observed period. For adjacent layers, the minimum angle is 32°. As the experimental MD curve crosses zero at normal emission, the sine-shaped fitting function with a periodicity of 18° will reach the maximum value at angles around ±5° (at 1/4-th of period), in agreement

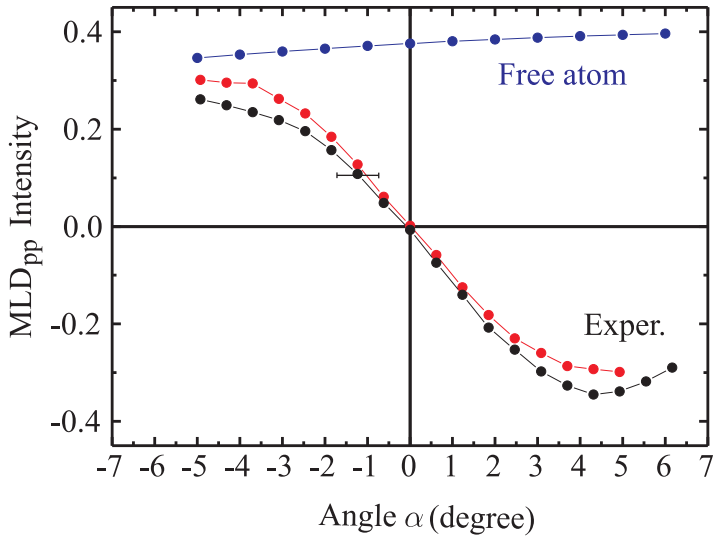

Figure 7.10: Angular dependence of the Gd-4f MD signal, given by the peak-to-peak amplitude (as shown in the Fig. 7.9); the MLD$_{pp}$ data points shown were derived from the data set in Fig. 7.7: experimental curve (black), its symmetrized average (red).

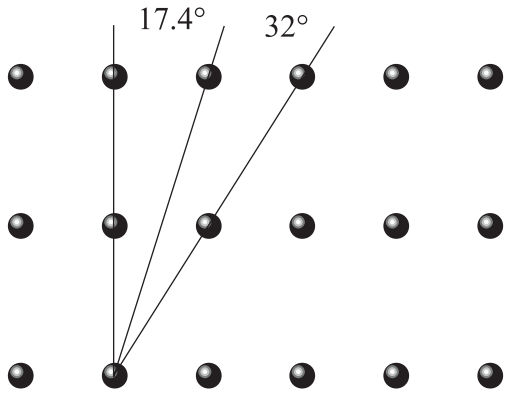

Figure 7.11: Perpendicular cut through the (0001) surface of an hcp lattice along the b-axis.

with the observed angular behavior.

7.3 $Eu(5 \times 5)/Gd(0001)$

Adsorption of Eu on the Gd(0001) surface and high-temperature annealing leads to the formation of a 5×5 superstructure that results in a sharp interface between the divalent europium layer and the trivalent gadolinium substrate [43]; a corresponding LEED pattern is shown in Fig. 7.12(a). Figure 7.12(b)

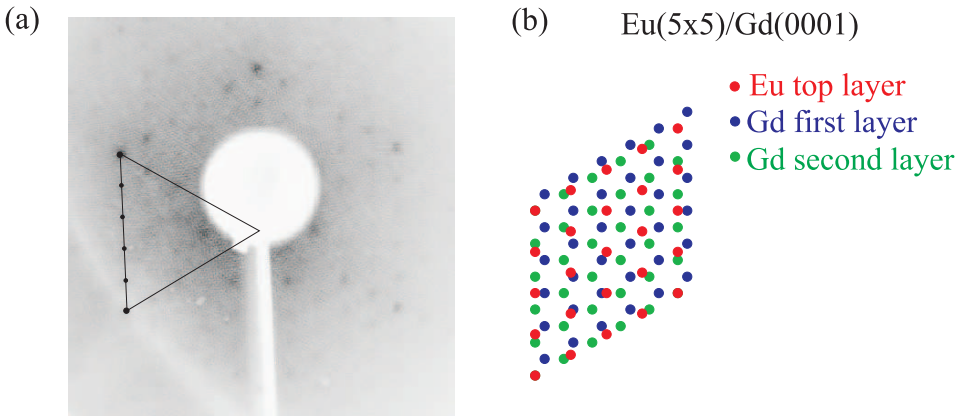

Figure 7.12: (a) LEED pattern corresponding to the $Eu(5\times5)/Gd(0001)$ surface superstructure recorded at $E_{kin} = 60$ eV ($\theta^{h\nu} = 30°$). (b) Positions of the Eu and Gd atoms in the first three layers corresponding to the $Eu(5\times5)/Gd(0001)$ supercell.

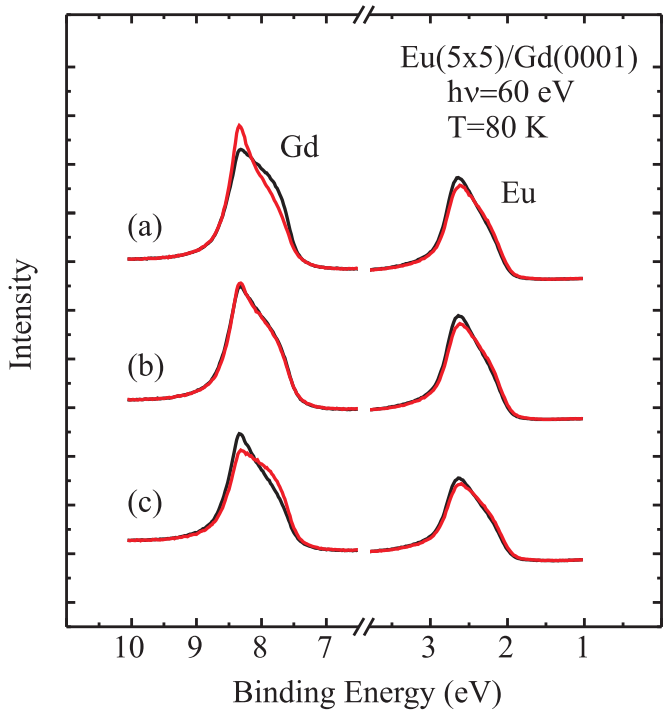

Figure 7.13: Eu-4f and Gd-4f PE spectra of the $Eu(5 \times 5)/Gd(0001)$ surface for two opposite magnetization directions (red and black curves), taken with linearly polarized light. Emission angle with respect to normal emission: (a) α =+3°, (b) α =0°, (c) α =-3°.

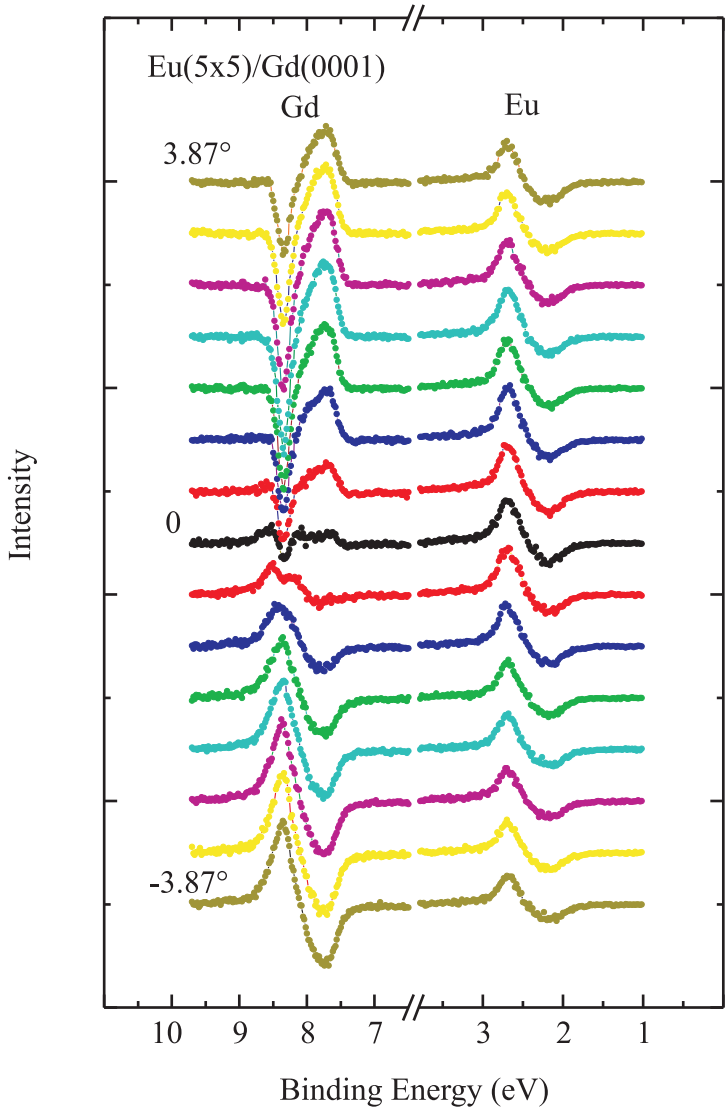

Figure 7.14: Series of Eu-4f and Gd-4f MLD spectra of $Eu(5 \times 5)/Gd(0001)$, representing the angular dependence in the region from $3° \leq \alpha \leq 3°$, with constant angular steps of 0.55°. The spectra were vertically offset for clarity.

illustrates the positions of the Eu atoms in the (5×5) supercell with respect to the first two Gd layers. This system represents a good model case to study photoelectron diffraction effects in MLD owing to the large energy separation between the Eu and Gd 4f spectra. One could expect that the photoelectron diffractions effects in the MD signal of the Eu 4f spectrum will be smeared out, due to the large number of non-equivalent adsorption sites of the Eu atoms (with respect to the underlying Gd layers).

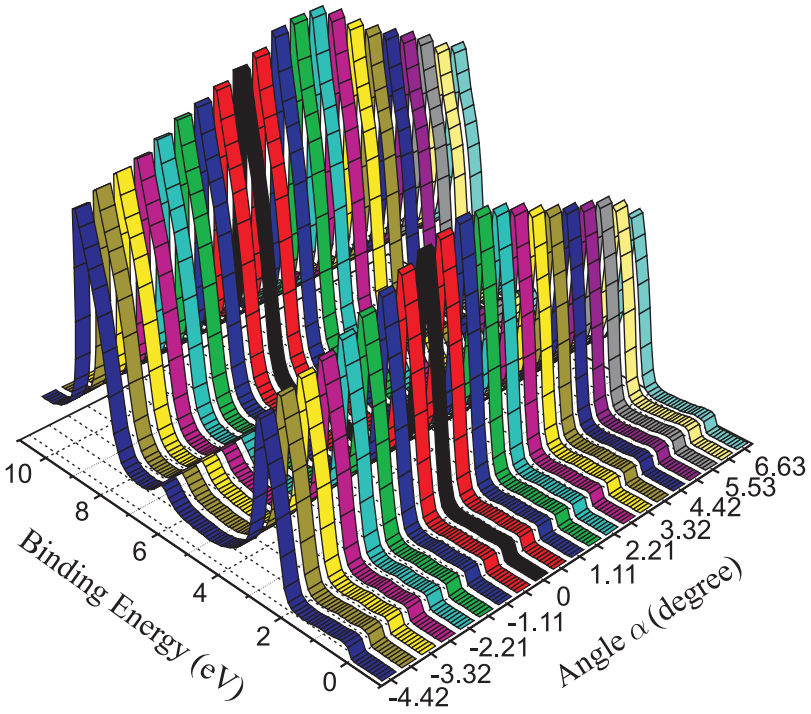

Figure 7.15: Set of sum spectra which represent the non-magnetic components of the Eu-4f and Gd-4f spectra of the $Eu(5 \times 5)/Gd(0001)$ interface, supplementing the set of spectra in Fig. 7.14, with the same color code for the emission angle α.

Figure 7.13 presents Eu-4f and Gd-4f photoemission spectra of $Eu(5 \times 5)/Gd(0001)$ at emission angles of $\alpha = -2.76°$, $0°$, $2.76°$; and opposite directions of magnetization. The 4f PE spectra of the surface Eu atoms and the bulk Gd atoms are clearly resolved. Similar to the MD behavior of Gd(0001) and $p(1 \times 1)O/Gd(0001)$ considered above, the Gd MLD component reverses sign upon crossing the normal emission direction, whereas the Eu MLD signal clearly has the same sign in all three spectra.

Figure 7.14 shows the data set of MLD spectra for various emission angles around surface normal, with constant angular steps of $0.55°$. The Eu surface and Gd bulk dichroic signals reveal a clearly different behavior: the dichroic signal of the Gd-4f spectrum varies rapidly with the angle around the surface normal. In contrast to that, the Eu spectrum shows only a slight modulation. The associated sum spectra are given in Fig. 7.15, indicating a smooth modulation of the intensity with a maximum near normal emission.

The peak-to-peak ratios for the Eu and Gd MLD components are presented in Fig. 7.16; they have been derived analogously as for $p(1 \times 1)O/Gd(0001)$, see above. The Eu MLD spectrum shows has a smooth angular dependence, similar to the free-atom case, indicating that the expected averaging of the phases indeed occurs. By contrast, the behavior of Gd MLD intensity resembles very closely the above presented cases, owing to the regular crystal periodic-

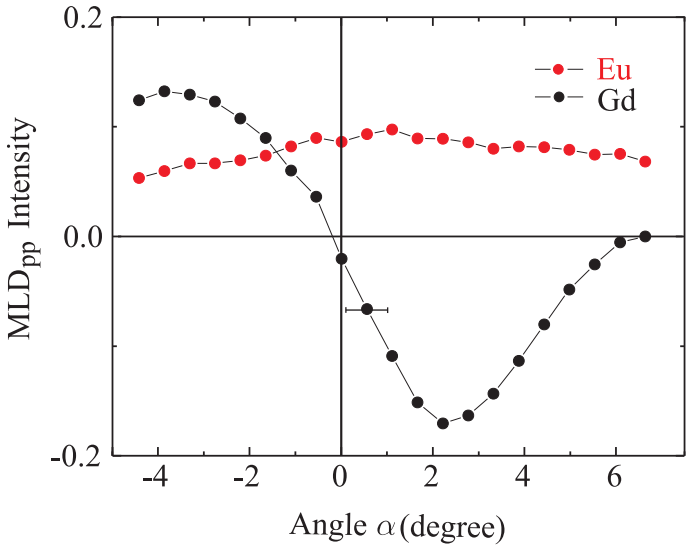

Figure 7.16: Angular dependences of the peak-to-peak amplitudes of the Eu (red) and Gd (black) 4f MLD signals derived from the data set shown in Fig. 7.14.

ity, though its detailed angular behavior is different; such differences can be expected as the result of a different structure of the top layer.